

Note

Grid Generation for Inlet Configurations Using Conformal Mapping

An orthogonal grid generation method for inlet geometries is developed using conformal mapping. In this method, the region on the physical plane is mapped onto the computational plane by one or two steps of conformal mapping; the mapping functions are determined numerically. A simple extension of this method allows the generation of three-dimensional grids for asymmetric geometries. Grids of *H*-type are also generated through the fundamental mapping function for *C*-type grids. © 1985 Academic Press, Inc.

1. INTRODUCTION

In this paper, a technique to generate orthogonal grids for inlet and inlet-centerbody configurations is proposed. The grids are intended to be suitable for use with finite volume transonic calculation and conformal mapping is employed to generate them.

The problems for inlet and inlet-centerbody configurations have been treated by Arlinger [1] and Ives and Menor [2], respectively. In the methods developed by these authors, the region exterior to the inlet (or inlet-centerbody) configuration is mapped onto a near circle. The near circle is then mapped to a unit circle. However, the mapping to the final near circle needs a number of sequential steps. The method described here maps the region on the physical plane onto a rectilinear strip through one or two transformations. This method is also applied to exhaust nozzle configurations.

2. ONE-STEP METHOD

2.1. Fundamental Mapping (*C*-Type Grids)

We consider a transformation function which maps the region of the physical plane ($z = x + iy$ plane) shown in Fig. 1 onto an rectilinear strip $0 \leq \eta \leq 1$ on the computational plane ($\zeta = \xi + i\eta$ plane) (Fig. 2). It is assumed: (1) the boundaries of the region on z plane $y = y_1(x)$ and $y = y_2(x)$ along the curves *ABC* and *FED* are given by two sets of data $z_{1n} = x_{1n} + iy_{1n}$ ($2 \leq n \leq n_1 - 1$) and $z_{2n} = x_{2n} + iy_{2n}$ ($2 \leq n \leq n_2 - 1$), (2) x_2 takes the minimum x_{2n_3} at $n = n_3$. The mapping function is assumed to have the form

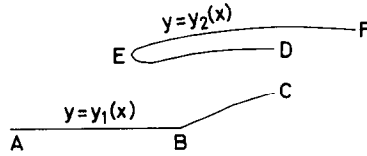


FIG. 1. Physical plane (z plane).

$$z = h \left[\zeta - \frac{1}{\pi} (e^{-\pi\zeta} + 1) \right] + A_1 + iB_1 + \sum_{k=2}^K \left[A_k \sin \frac{(k-1)\pi(\zeta - \zeta_0)}{L} + iB_k \cos \frac{(k-1)\pi(\zeta - \zeta_0)}{L} \right], \quad (1)$$

where $h; A_k, B_k$ ($1 \leq k \leq K$); ζ_0 and L are unknown real constants to be determined. When $A_k = B_k = 0$ ($1 \leq k \leq K$), the expression (1) gives the transformation function which maps the upper half plane $y \geq 0$ with a cut $y = h$ ($x \geq 0$) onto the rectilinear strip $0 \leq \eta \leq 1$ on ζ plane.

Putting $\eta = 0$ and 1 in (1) and writing the real and imaginary parts separately, we get on $\eta = 0$,

$$x = x1(\xi) = h \left[\xi - \frac{1}{\pi} (e^{-\pi\xi} + 1) \right] + A_1 + \sum_{k=2}^K A_k \sin \frac{(k-1)\pi(\xi - \xi_0)}{L}, \quad (2)$$

on $\eta = 1$,

$$x = x2(\xi) = h \left[\xi + \frac{1}{\pi} (e^{-\pi\xi} - 1) \right] + A_1 + \sum_{k=2}^K \left[A_k \cosh \frac{(k-1)\pi}{L} + B_k \sinh \frac{(k-1)\pi}{L} \right] \sin \frac{(k-1)\pi(\xi - \xi_0)}{L}, \quad (3)$$

on $\eta = 0$,

$$y1 = B_1 + \sum_{k=2}^K B_k \cos \frac{(k-1)\pi(\xi - \xi_0)}{L}, \quad (4)$$

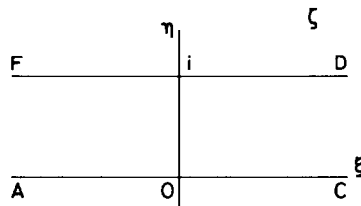


FIG. 2. Computational plane (ζ plane).

and on $\eta = 1$,

$$y_2 = h + B_1 + \sum_{k=2}^K \left[A_k \sinh \frac{(k-1)\pi}{L} + B_k \cosh \frac{(k-1)\pi}{L} \right] \times \cos \frac{(k-1)\pi(\xi - \xi_0)}{L}. \quad (5)$$

The expressions (4) and (5) mean the assumption that y_1 and y_2 are even periodic functions of $t = \xi - \xi_0$ with a period $2L$. The unknown constants are determined by following iterative method of solution.

The n th approximations for h, A_k, B_k, ξ_0, L are assumed to be known.

(i) Substitution of these values in (2) and (3) gives the $(n+1)$ th approximations of x_1 and x_2 .

(ii) Find $\xi = \xi_{n3}$ which makes $x_2(\xi)$ minimum and determine A_1 so that $x_2(\xi_{n3}) = x_{2n3}$.

(iii) Obtain the solutions of $x_1(\xi) = x_{12}$ and $x_2(\xi) = x_{22}$ and take the smaller as ξ_1 .

(iv) Obtain the solutions of $x_1(\xi) = x_{2n1-1}$ and $x_2(\xi) = x_{2n2-1}$ and take the larger as ξ_2 .

(v) Determine $z_1(\xi_1) = z_{11}, z_2(\xi_1) = z_{21}, z_1(\xi_2) = z_{1n1},$ and $z_2(\xi_2) = z_{2n2}$ by extrapolation. The procedure (i)–(vi) defines $x_1(\xi)$ and $x_2(\xi)$ for the interval

$$\xi_1 \leq \xi \leq \xi_2 = \xi_1 + L. \quad (6)$$

(vi) Put $L = \xi_2 - \xi_1$ and $\xi_0 = \xi_1$.

(vii) Though the left-hand sides of (4) and (5) y_1 and y_2 are originally given as functions of x , they are regarded as functions of ξ for the interval (6) through the functions $x_1(\xi)$ and $x_2(\xi)$. The constants h, A_k ($2 \leq k \leq K$) and B_k ($1 \leq k \leq K$) are determined by the Fourier analysis. The relations

$$B_1 = \frac{1}{L} \int_0^L y_1(t) dt,$$

$$B_k = \frac{2}{L} \int_0^L y_1(t) \cos \frac{(k-1)\pi t}{L} dt,$$

$$h = \frac{1}{L} \int_0^L y_2(t) dt - B_1$$

and

$$A_k = \left(1 / \sinh \frac{(k-1)\pi}{L} \right) \left[\frac{2}{L} \int_0^L y_2(t) \cos \frac{(k-1)\pi t}{L} dt - B_k \cosh \frac{(k-1)\pi}{L} \right]$$

$$(2 \leq k \leq K),$$

where $t = \xi - \xi_0$, are used.

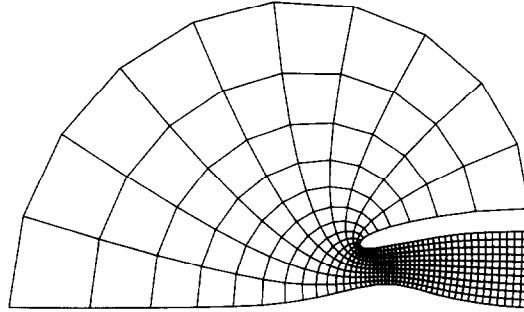


FIG. 3. Example of C-type grid (1). $n_1 = 19$, $n_2 = 25$, $K = 40$, $r = 0.5$.

(viii) All of the $(n + 1)$ th approximations $\phi^{(n+1)}$ thus obtained are replaced by $(1 - r)\phi^{(n)} + r\phi^{(n+1)}$, where r is a relaxation constant, typically 0.5. This prevents the divergence of the successive approximation. The procedure (i)–(viii) is repeated until the required convergence is attained. The first approximation is given by $h = y2_{n3}$, $A_k = B_k = 0$ ($1 \leq k \leq K$), $\xi_1 = 0$, $L = x1_{n1-1} - x1_2$, for example. Through the calculation, the use of double precision is recommended because the hyperbolic functions included take very large values for large k .

The curves of constant ξ and η on z plane give the grids of C-type. The examples of the grids generated by this method are shown in Figs. 3 and 4. It is not difficult to choose the values of ξ so that two different geometric grids match along a common line, leading to the generation of grids suitable for three-dimensional asymmetric inlet flow analyses [2]. An example of two matched planer grids is shown in Fig. 5. The grid for the lower geometry was developed choosing the values of ξ so as to match that of the upper geometry along the centerline.

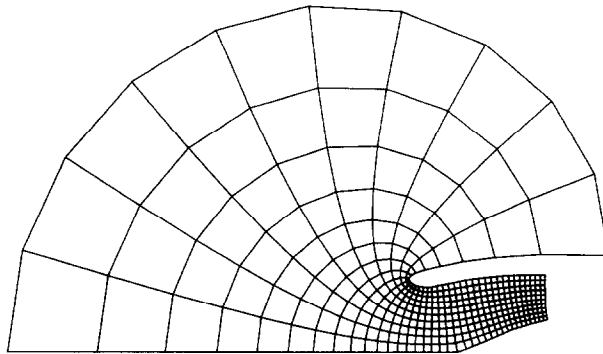


FIG. 4. Example of C-type grid (2). $n_1 = 22$, $n_2 = 25$, $K = 40$, $r = 0.5$.

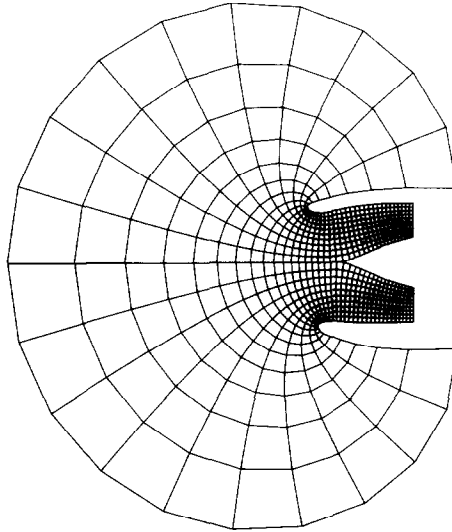


FIG. 5. Orthogonal grids matched along the centerline.

2.2. *H*-Type Grids

Once the function (1) is determined, it is utilized to generate an *H*-type grid suitable for the calculation of the flows in boundary layers or mixing zones of exhaust nozzles. The rectilinear strip $0 \leq \eta \leq 1$ on ζ plane is mapped onto the upper half $Y \geq 0$ of $Z = X + iY$ plane with a cut $Y = 1$ ($X \geq 0$) by

$$Z = X + iY = \zeta - \zeta_s - \frac{1}{\pi} [\exp\{-\pi(\zeta - \zeta_s)\} + 1]. \quad (7)$$

The point $\zeta_s = \xi_s + i$ corresponds to the branch point z_s given arbitrarily on *DEF* on z plane. The lines of constant X or Y on z plane give the *H*-type grid. Equation (7) cannot be solved explicitly for ζ corresponding to given Z and iterative method must be employed. Attention is paid to that $(dZ/d\zeta)(\zeta_s) = 0$. Examples are shown in Figs. 6 and 7 for the *H*-type grids generated by this method.

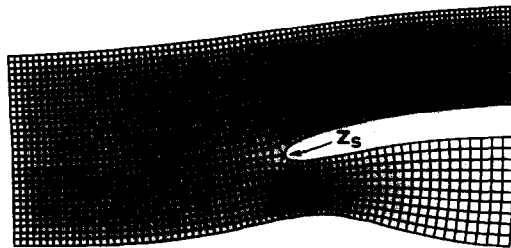


FIG. 6. *H*-type grid for the inlet same as shown in Fig. 3.

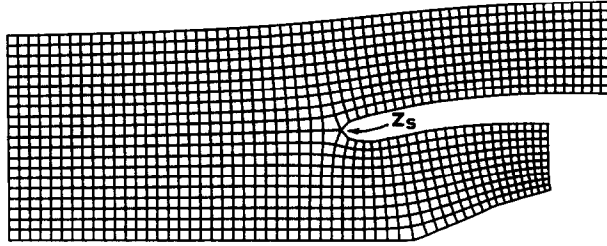


FIG. 7. *H*-type grid for the inlet same as shown in Fig. 4.

3. TWO-STEP METHOD

The one-step method described in the preceding section is applied even when the configuration has a sharp angle at *B* as the example shown in Fig. 4. But when the angle is nearly right angle, as the case for a blunt-nosed centerbody, the resolution of the mapping diminishes around there. In this case, the two-step method described hereafter is useful.

3.1. Fundamental Mapping (*C*-Type Grids)

First, we map the region *ABCDEF* on *z* plane (Fig. 8) onto the rectilinear strip $0 \leq \eta \leq 1$ on ζ plane (Fig. 9) by

$$z = h \left[\zeta - \frac{1}{\pi} (e^{-\pi\zeta} + 1) \right] + A_1 + \sum_{k=2}^{K_1} A_k \sin \frac{(k-1)\pi(\zeta - \xi_0)}{L_1}. \quad (8)$$

The constants h, A_k, ξ_0, L_1 are determined in a manner similar to that in the preceding section. The relation (8) is obtained by putting $B_k = 0$ ($k \geq 1$) in (1) and gives the transformation function for the inlets without centerbodies. We denote the image of the arc *BC* on ζ plane by

$$\eta = \eta_1(\xi) \quad (\xi_3 \leq \xi \leq \xi_4).$$

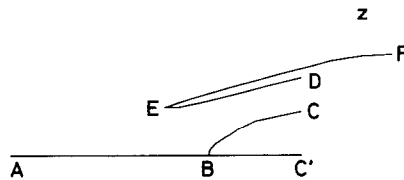


FIG. 8. Physical plane (*z* plane). Inlet configuration having an acute corner at *B*.

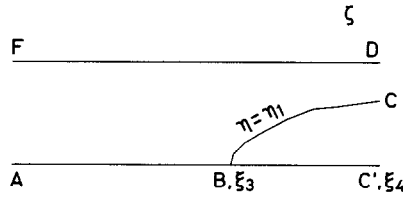


FIG. 9. First step mapping onto ζ plane.

Next, the region $ABCDEF$ on ζ plane (Fig. 9) is mapped onto the semi-infinite strip $0 \leq u, 0 \leq v \leq 1$, on $w = u + iv$ plane (Fig. 10) by

$$\zeta = \frac{2}{\pi} \log \cosh \frac{\pi w}{2} + B_0 + \sum_{k=1}^{K_2} B_k \cos \frac{(2k-1)\pi(w-i)}{2L_2}. \tag{9}$$

It is supposed that the points B ($\zeta = \xi_3$) and C ($\zeta = \xi_4 + i\eta_4$) are mapped to the origin $w = 0$ and $w = L_2$, respectively. The unknown constants B_k ($0 \leq k \leq K_2$) and L_2 are determined similarly as in the preceding section. We have at $v = 0$,

$$\xi = \frac{1}{\pi} \log \cosh^2 \frac{\pi u}{2} + B_0 + \sum_{k=1}^{K_2} B_k \cosh \frac{(2k-1)\pi}{2L_2} \cos \frac{(2k-1)\pi u}{L_2}$$

and

$$\eta = \eta_1(\xi) = \sum_{k=1}^{K_2} B_k \sinh \frac{(2k-1)\pi}{2L_2} \sin \frac{(2k-1)\pi u}{L_2}. \tag{10}$$

This leads to

$$B_k = \left(2/L_2 \sinh \frac{(2k-1)\pi}{2L_2} \right) \int_0^{L_2} \eta_1 \sin \frac{(2k-1)\pi u}{2L_2} du \quad (1 \leq k \leq K_2).$$

Correspondence of the point B to $w = 0$ gives

$$B_0 = \xi_3 - \sum_{k=1}^{K_2} B_k \cosh \frac{(2k-1)\pi}{2L_2}.$$

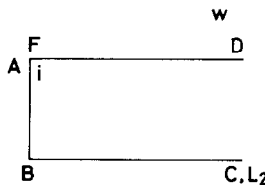


FIG. 10. Second step mapping onto w plane.

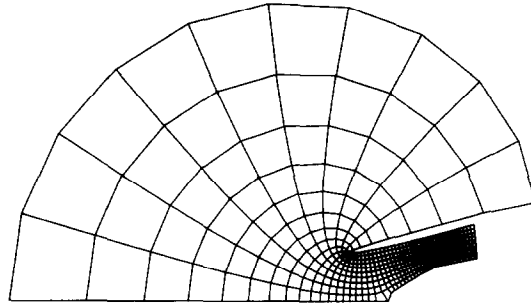


FIG. 11. Example of C-type grid generated by two-step method. $n_1 = 10$, $n_2 = 18$, $K_1 = 40$, $r_1 = 0.5$, $K_2 = 20$, $r_2 = 0.1$.

The relation (10) indicates the assumption made: $\eta_1(u)$ is an odd periodic function with a period $4L_2$ and is symmetric about $u = L_2$.

The semi-infinite strip $CBAFED$ on w plane is mapped onto the infinite strip $0 \leq \eta_2 \leq 1$ on $\zeta_2 = \xi_2 + i\eta_2$ plane by

$$w = \frac{2}{\pi} \operatorname{arccosh} \exp \left(\frac{\pi \zeta_2}{2} \right).$$

The lines of constant ξ_2 or η_2 give the C-type grid on z plane. An example of C-type grid generated by this method is given in Fig. 11.

3.2. H-Type Grids

We generate an H-type grid on z plane, using the transformation functions (8) and (9). We denote by z_s the branch point which is given arbitrarily on DEF on z plane. The infinite strip on ζ_2 plane $0 \leq \eta_2 \leq 1$ is mapped onto the upper half $Y_2 \geq 0$ of $Z_2 = X_2 + iY_2$ plane with a cut $Y_2 = 1$ ($X_2 \geq 0$) by

$$Z_2 = \zeta_2 - \zeta_{2s} - \frac{1}{\pi} [\exp\{-\pi(\zeta_2 - \zeta_{2s})\} + 1], \tag{11}$$

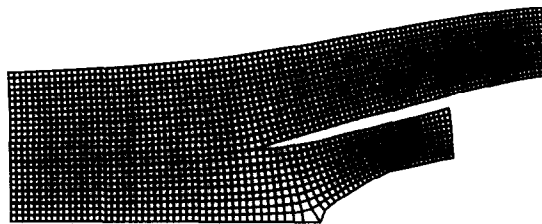


FIG. 12. H-type grid for the configuration same as shown in Fig. 11.

where $\zeta_{2_s} = \zeta_{2_s} + i$ is the image of z_s on ζ_2 plane. The curves of constant X_2 or Y_2 on z plane give an H -type grid. The transformation (11) cannot be solved explicitly for ζ_2 and successive approximation must be employed to obtain the value of ζ_2 corresponding to given Z_2 . Attention is also paid to that $(dZ_2/d\zeta_2)(\zeta_{2_s}) = 0$. Figure 12 shows the H -type grid generated by the present method for the same configuration as shown in Fig. 11.

REFERENCES

1. B. G. ARLINGER, *AIAA J.* **13** (1975), 1614.
2. D. C. IVES AND W. A. MENOR, AIAA Paper 81-0997, New York, 1981.

RECEIVED: November 15, 1983; REVISED: April 10, 1984

KENJI INOUE

*National Aerospace Laboratory,
Jindaiji, Chofu, Tokyo 182, Japan*